Dynamics of one-dimensional Heisenberg spin glasses in the high-field limit

A. Boukahil and D. L. Huber*
Synchrotron Radiation Center, 3731 Schneider Drive, Stoughton, Wisconsin 53589
(Received 9 February 1994)

This paper reports the results of a study of the distribution and localization of the magnon modes in one-dimensional Heisenberg spin glasses with nearest-neighbor interactions. The analysis is limited to high fields and frequencies near the precession frequency. Both symmetric and asymmetric distributions of exchange interactions of the form $P(J) \propto |J|^{-\alpha}$ ($\alpha < 1$) are treated in detail. The results of approximate calculations based on the coherent-exchange approximation are shown to be in good agreement with numerical data obtained by applying mode-counting techniques to arrays of 10^7 spins. Particular emphasis is placed on the qualitative differences in the behavior that arise depending on whether the average values of J^{-1} and J^{-2} are zero, nonzero, or infinite.

I. INTRODUCTION

In a recent paper (hereafter referred to as I),[1] the results of a detailed study of the magnon excitations in a one-dimensional Heisenberg spin glass were reported. An analysis was carried out in the zero-field and high-field limits for a model where the nearest-neighbor exchange interactions had the values $+1$ and -1, with probabilities $1-c$ and c, respectively, there being no correlation between different bonds. In the high-field limit, the results of computer simulation studies were compared with the predictions of an analytical theory based on the coherent-exchange approximation (CEA). Although the CEA did not account for the fine structure at high frequencies in the density of states and the inverse localization length, it did prove to be an accurate approximation near the precession frequency over the full range of c. The purpose of this paper is to extend the study of the dynamics of one-dimensional spin glasses in high fields to a more general class of interactions than that of the $\pm J$ model.

Our interest in this paper is in Heisenberg spin systems where the nearest-neighbor exchange interactions have continuous distributions of the form

$$P(J) \propto |J|^{-\alpha}, \quad \alpha < 1 , \tag{1.1}$$

with no correlation between different bonds. We limit the analysis to saturating magnetic fields and consider two cases: symmetric distributions where $P(J)=P(-J)$, and asymmetric distributions for which, in general, $P(J) \neq P(-J)$. Both the integrated density of states and the inverse localization length are calculated in the CEA and the results compared with corresponding data obtained by applying mode counting techniques to chains of 10^7 spins. The major result to emerge from our study is that, as in the case of the $\pm J$ model studied in Ref. 1, the CEA provides a quantitatively accurate (albeit approximate) description of the distribution and localization of the magnon modes in the vicinity of the precession frequency.

The starting point in the analysis is the set of equations of motion for the transverse spin operators S_{+j} which are obtained from the Heisenberg Hamiltonian

$$\mathcal{H} = -H \sum_j S_{zj} - \sum_j J_{j,j+1} \mathbf{S}_j \cdot \mathbf{S}_{j+1} . \tag{1.2}$$

In saturating fields, where the expectation value of S_{zj} can be replaced by 1, the linearized equations of motion take the form ($\hbar = 1$)

$$i\, dS_{+j}/dt = (J_{j-1,j} + J_{j,j+1} + H) S_{+j} - J_{j-1,j} S_{+j-1} - J_{j,j+1} S_{+j+1} . \tag{1.3}$$

Assuming a harmonic time dependence, $\exp(-i\omega t)$, and taking the zero of energy to be the spin precession frequency, H, we obtain the resulting equation for the spin amplitudes U_j

$$(J_{j-1,j} + J_{j,j+1} - E) U_j = J_{j-1,j} U_{j-1} + J_{j,j+1} U_{j+1} , \tag{1.4}$$

where $E = \omega - H$. Note that since the analysis is carried out on chains of N spins, one has $U_0 = U_{N+1} = J_{0,1} = J_{N,N+1} \equiv 0$.

As pointed out elsewhere,[2] one obtains the integrated density of states from a Sturm sequence made up from the determinants associated with Eq. (1.4). If we denote the determinant characterizing the equations of motion of a chain of j spins by D_j, the D_j obeys the recursion relation

$$D_j(E) = (J_{j-1,j} + J_{j,j+1} - E) D_{j-1}(E) - J_{j-1,j}^2 D_{j-2}(E) . \tag{1.5}$$

Writing $R_j = D_j / D_{j-1}$, one has the equivalent expression

$$R_j(E) = J_{j-1,j} + J_{j,j+1} - E - J_{j-1,j}^2 / R_{j-1}(E) . \tag{1.6}$$

The integrated density of states, denoted by $I_{\mathrm{DOS}}(E)$, is given by the number of negative terms in the sequence $R_1(E), R_2(E), \ldots, R_N(E)$, where N is the number of spins in the array.

The spatial extent of the modes is characterized by the

 ©1994 The American Physical Society

inverse localization length which is calculated from the amplitude ratio $T_j = U_{j+1}/U_j$. From Eq. (1.4), $T_j(E)$ can be written

$$J_{j,j+1}T_j(E) = J_{j-1,j} + J_{j,j+1} - E - J_{j-1,j}/T_{j-1}(E) . \tag{1.7}$$

In units of the inverse of the lattice constant, the inverse localization length associated with modes of energy E, $I_{\rm ILL}(E)$, is given by[3]

$$L_{\rm ILL}(E) = (1/N)\sum_{j=1}^{N} \ln|T_j(E)| . \tag{1.8}$$

We note, in passing, that since the signs of $J_{j-1,j}$ and $J_{j,j+1}$ can differ, the amplitude ratios, $T_j(E)$, are not a Sturm sequence.[4] As a consequence, the integrated density of states is not related to the number of negative terms in the sequence $T_1(E), T_2(E), \ldots, T_N(E)$, a result we have confirmed by direct calculation.

II. CEA AND THE CONVENTIONAL REGIME

In this section, we summarize the CEA and use it to obtain the integrated density of states and the inverse localization length in what we refer to as the "conventional regime." In the CEA, the effect of the disorder on the configurationally averaged single-particle Greens function is accounted for by a complex, energy-dependent exchange integral, $J_c(E)$, which is obtained as the solution to the equation.[1,5]

$$\int dJ\, P(J)[J - J_c(E)]/\{1 - [J - J_c(E)]\Gamma(E)\} = 0 , \tag{2.1}$$

where $P(J)$ denotes the distribution of exchange integrals. In one dimension, $\Gamma(E)$ has the form

$$\Gamma(E) = -1/J_c(E) + [E/J_c(E)][E^2 - 4EJ_c(E)]^{-1/2} . \tag{2.2}$$

The corresponding single-site Greens function is expressed as

$$G_0(E) = [E^2 - 4EJ_c(E)]^{-1/2} . \tag{2.3}$$

The magnon density of states, $\rho(E)$, is related to the imaginary part of G_0 through the equation

$$\rho(E) = -\pi^{-1}\,{\rm Im}G_0(E + i\varepsilon) , \tag{2.4}$$

while the integrated density of states per spin is expressed as

$$I_{\rm DOS}(E)/N = -\pi^{-1}\int_0^E dE'\,{\rm Im}G_0(E' + i\varepsilon) . \tag{2.5}$$

Note that with this definition, $I_{\rm DOS}(E)$ is the integrated density of states referenced to the value at $E = 0$. In one dimension, the inverse localization length is related to the integral of the real part of the Greens function.[1,3] In particular, we have

$$L_{\rm ILL}(E) = \int_0^E dE'\,{\rm Re}G_0(E' + i\varepsilon) . \tag{2.6}$$

Equations (2.5) and (2.6), with G_0 evaluated according to Eq. (2.3), give the CEA results for the integrated density of states and the inverse localization length. What we refer to as the conventional regime pertains to situations where the integrals $\int dJ\, P(J)J^{-1}$ and $\int dJ\, P(J)J^{-2}$ are finite. To see the consequences of this at low frequencies, we keep only the lowest-order terms in $\Gamma(E)$ and $G_0(E)$.

$$\Gamma(E) \approx -1/J_c - iE^{1/2}J_c^{-3/2}/2 , \tag{2.7}$$

$$G_0(E) \approx -iE^{-1/2}J_c^{-1/2}/2 . \tag{2.8}$$

The self-consistent equation for J_c takes the form

$$1/J_c + iE^{1/2}J_c^{-3/2}/2 - \int dJ\, P(J)/(J - W) , \tag{2.9}$$

with $W = iE^{1/2}J_c^{1/2}/2$. Assuming that the average values of J^{-1} and J^{-2} are not infinite, one can expand the integral in (2.9) and obtain the equation

$$1/J_c + iE^{1/2}J_c^{-3/2}/2 = \langle J^{-1}\rangle + W\langle J^{-2}\rangle , \tag{2.10}$$

where $\langle J^{-n}\rangle = \int dJ\, P(J)J^{-n}$.

In the case of a symmetrical distribution, one has $\langle J^{-1}\rangle = 0$. For small $|E|$, the second term on the left-hand side of (2.10) can be neglected (as may be verified *ex post facto*) so that we obtain

$$J_c(E)^{-3/2} = i|E|^{1/2}\langle J^{-2}\rangle/2 , \tag{2.11}$$

from which it follows

$$G_0(E) = e^{-i\pi/3}2^{-4/3}|E|^{-1/3}\langle J^{-2}\rangle^{1/3} . \tag{2.12}$$

As a consequence, the integrand density of states and the inverse localization length are given by

$$I_{\rm DOS}(E)/N = \pi^{-1}(3/2^{7/3})|E|^{2/3}\langle J^{-2}\rangle^{1/3}\sin(\pi/3) , \tag{2.13}$$

and

$$L_{\rm ILL}(E) = (3/2^{7/3})|E|^{2/3}\langle J^{-2}\rangle^{1/3}\cos(\pi/3) . \tag{2.14}$$

In (2.13), it is understood that $I_{\rm DOS}(E)$ for $E < 0$, is the number of modes in the interval between E and zero.

In the case of asymmetric distributions, $\langle J^{-1}\rangle \neq 0$, so that for $E > 0$ one has

$$1/J_c + iE^{1/2}J_c^{-3/2}/2 = \langle J^{-1}\rangle + iE^{1/2}J_c^{1/2}\langle J^{-2}\rangle/2 , \tag{2.15}$$

which is equivalent to

$$1/J_c(E) = \langle J^{-1}\rangle + iE^{1/2}\langle J^{-1}\rangle^{-1/2}(\langle J^{-2}\rangle - \langle J^{-1}\rangle^2)/2 . \tag{2.16}$$

As a consequence, G_0 is given by

$$G_0(E) = -(i/2)[\langle J^{-1}\rangle/E]^{1/2} + (1/8)[(\langle J^{-2}\rangle - \langle J^{-1}\rangle^2)/\langle J^{-1}\rangle] . \tag{2.17}$$

The resulting expressions for the integrated density of states and the inverse localization length take the form

$$I_{\mathrm{DOS}}(E)/N=\pi^{-1}\langle J^{-1}\rangle^{1/2}E^{1/2}\ , \tag{2.18}$$

and

$$L_{\mathrm{ILL}}(E)=(1/8)[(\langle J^{-2}\rangle-\langle J^{-1}\rangle^2)/\langle J^{-1}\rangle]E\ . \tag{2.19}$$

These equations assume $\langle J^{-1}\rangle$ and E are both positive. If they differ in sign, then the L_{ILL} is inferred from $I_{\mathrm{DOS}}(-E)$ via

$$L_{\mathrm{ILL}}(E)=|\langle J^{-1}\rangle|^{1/2}|E|^{1/2},|E|\to 0\ , \tag{2.20}$$

while the integrated density of states varies more rapidly than $|E|$.

Equations (2.13), (2.14), (2.18), and (2.19) generalize the results obtained in I for the $\pm J$ model. They show that in the conventional regime, the power-law behavior of $I_{\mathrm{DOS}}(E)$ and $L_{\mathrm{ILL}}(E)$ are independent of the details of the distribution. In the following section, the predictions of the CEA for the continuum distribution with $\alpha=-2$ will be compared with the corresponding simulation data.

III. CEA RESULTS AND NUMERICAL SIMULATION STUDIES

A. Symmetric distributions

The normalized distribution for the exchange integral is given by

$$P(J)=(1-\alpha)2^{-\alpha}|J|^{-\alpha},\quad -\tfrac{1}{2}\le J\le\tfrac{1}{2}\ . \tag{3.1}$$

For $\alpha<-1$, one has

$$\langle J^{-2}\rangle=-4(1-\alpha)/(\alpha+1)\ . \tag{3.2}$$

In Fig. 1, we compare the simulation data with predictions of the CEA. The numerical studies were carried out on chains of 10^7 spins using Eqs. (1.6), (1.7), and (1.8), while the CEA results were obtained from Eqs. (2.13) and (2.14). From the figure, it is apparent that the CEA gives good results for both the I_{DOS} and the L_{ILL} over the range $10^{-4}\le E\le 1$.

The behavior in the interval $-1<\alpha<1$ that is predicted by the CEA follows from solving Eq. (2.9). One finds that the second term on the left-hand side can be neglected, leaving the equation

$$1/J_c=\int dJ\,P(J)/(J-iE^{1/2}J_c^{1/2}/2)\ . \tag{3.3}$$

A general analysis of (3.3) indicates that the solution is of the form

$$J_c=C(\alpha)|E|^{\alpha/(2-\alpha)}\exp[-i\pi/(2-\alpha)]\ , \tag{3.4}$$

where $C(\alpha)$ is independent of E. Thus, both I_{DOS} and L_{ILL} vary as $|E|^{(1-\alpha)/(2-\alpha)}$ with the ratio

$$L_{\mathrm{ILL}}(E)/(\pi/N)I_{\mathrm{DOS}}(E)=\cot[(\pi/2)(1-\alpha)/(2-\alpha)]\ . \tag{3.5}$$

For the values $\alpha=-\frac{1}{2}$, 0, and $\frac{1}{2}$, we find for the I_{DOS}

$$\alpha=-\tfrac{1}{2}$$

$$I_{\mathrm{DOS}}(E)/N=5\pi^{-3/5}2^{-6/5}3^{-3/5}\sin(3\pi/10)|E|^{3/5}\ , \tag{3.6}$$

$$\alpha=0$$

$$I_{\mathrm{DOS}}(E)/N=\pi^{-1/2}\sin(\pi/4)|E|^{1/2}\ , \tag{3.7}$$

$$\alpha=\tfrac{1}{2}$$

$$I_{\mathrm{DOS}}(E)/N=3\pi^{-1/3}2^{-4/3}\sin(\pi/6)|E|^{1/3}\ , \tag{3.8}$$

with the $L_{\mathrm{ILL}}(E)$ obtained with the help of Eq. (3.5). Figures 2, 3, and 4 show the comparison between the simulation data for chains of 10^7 spins and the predictions of the CEA. As in Fig. 1, the two are in very good agreement, particularly for $E\le 10^{-3}$.

The point $\alpha=-1$ marks the boundary between the

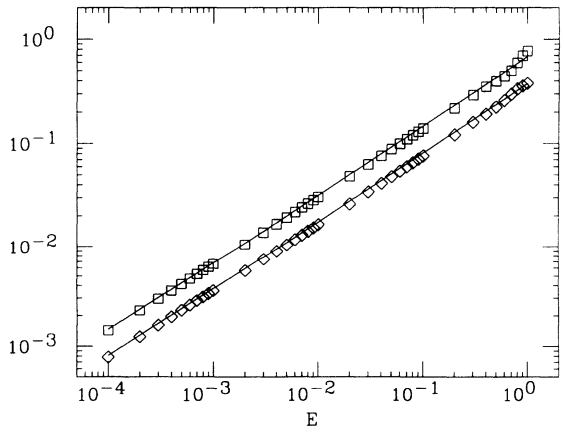

FIG. 1. Integrated density of states and inverse localization length for $\alpha=-2$. $\Diamond I_{\mathrm{DOS}}(E)/N$; $\Box L_{\mathrm{ILL}}(E)$. The straight lines are the CEA predictions given by Eqs. (2.13) and (2.14). Here, and in Figs. 2–8, the numerical data are from a single configuration of 10^7 spins.

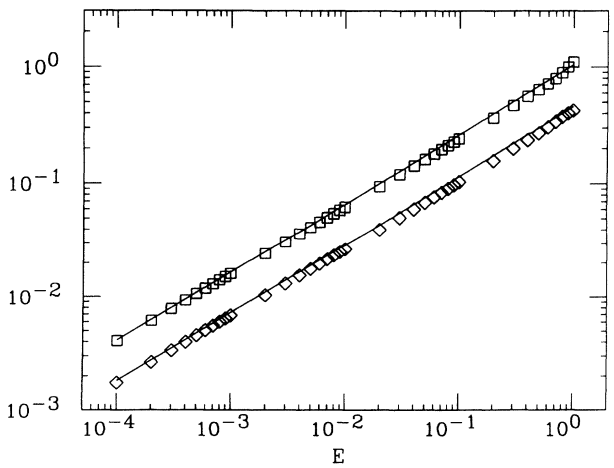

FIG. 2. Integrated density of states and inverse localization length for $\alpha=-\frac{1}{2}$. $\Diamond I_{\mathrm{DOS}}(E)/N$; $\Box L_{\mathrm{ILL}}(E)$. The straight lines are the CEA predictions obtained from Eqs. (3.5) and (3.6).

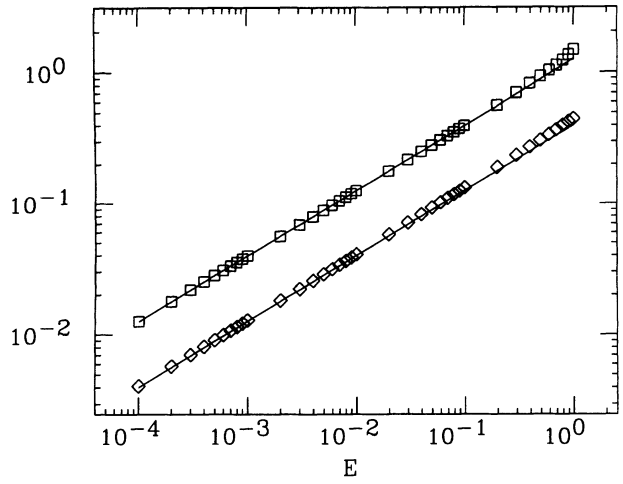

FIG. 3. Integrated density of states and inverse localization length for $\alpha=0$. $\Diamond I_{\rm DOS}(E)/N$; $\Box L_{\rm ILL}(E)$. The straight lines are the CEA predictions obtained from Eqs. (3.5) and (3.7).

conventional regime and the regime where the power dependence of $|E|$ is a function of α. A numerical solution of Eqs. (2.1), (2.2), and (2.3) shows that in the CEA, when $\alpha=-1$, both the integrated density of states and the inverse localization length vary as $|E|^{2/3}$ with slowly varying corrections. Similar to what happens when $\alpha\neq-1$, the CEA is in good agreement with the simulation near $E=0$ (see Fig. 5).

B. Asymmetric distributions

Here we consider the considerations of an asymmetric distribution of exchange interactions of the form

$$P(J)=C_1J^{-\alpha},\quad J>0\,,$$
$$C_2|J|^{-\alpha},\quad J<0\,, \tag{3.9}$$

with $C_1>C_2$. As noted in Sec. II, the CEA predicts conventional behavior for asymmetric distributions whenever both $\langle J^{-1}\rangle$ and $\langle J^{-2}\rangle$ are finite. This will be the case

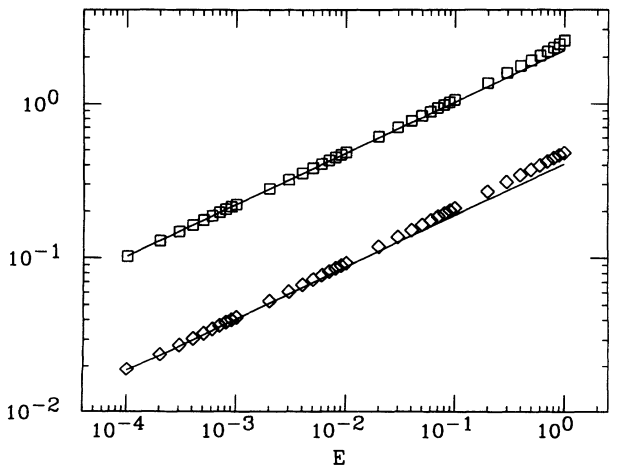

FIG. 4. Integrated density of states and inverse localization length for $\alpha=\frac{1}{2}$. $\Diamond I_{\rm DOS}(E)/N$; $\Box L_{\rm ILL}(E)$. The straight lines are the CEA predictions obtained from Eqs. (3.5) and (3.8).

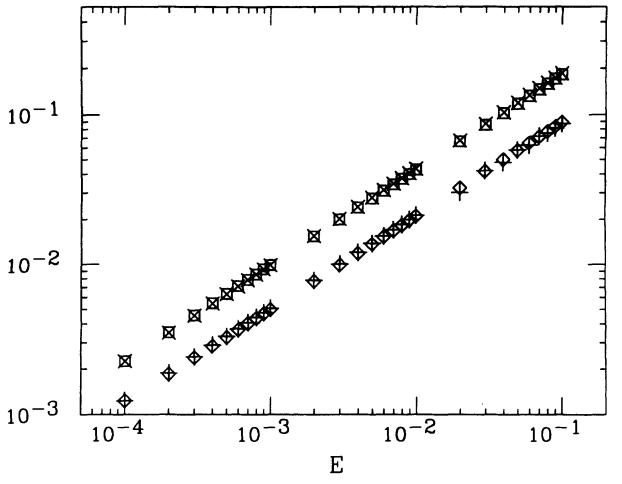

FIG. 5. Integrated density of states and inverse localization length for $\alpha=-1$. The simulation data are shown as open symbols: $\Diamond I_{\rm DOS}(E)/N$; $\Box L_{\rm ILL}(E)$. The CEA results are $+I_{\rm DOS}(E)/N$; $\times L_{\rm ILL}(E)$. The latter were obtained by solving Eqs. (2.1)–(2.3) and numerically integrating G_0 from 10^{-4} to E. The integral of G_0 from 0 to 10^{-4} was set equal to the value given by the simulation data.

for $\alpha<-1$. In Fig. 6, we show the CEA results and the numerical simulation data for $\alpha=-2$ and $C_1=3C_2$ for both $E>0$ and $E<0$. The CEA predictions for the integrated density of states and the inverse localization length for $E>0$ are obtained from Eqs. (2.18) and (2.19), while the predictions of the inverse localization length for $E<0$ follows from Eq. (2.20). In all cases, one has $\langle J^{-1}\rangle=\frac{3}{2}$ and $\langle J^{-2}\rangle=12$.

For $-1<\alpha<0$, $\langle J^{-1}\rangle$ is finite, but $\langle J^{-2}\rangle$ is infinite. To see the consequences of this, we write the self-consistent equation for J_c [Eq. (2.9) with the second term on the left-hand side omitted] in the form

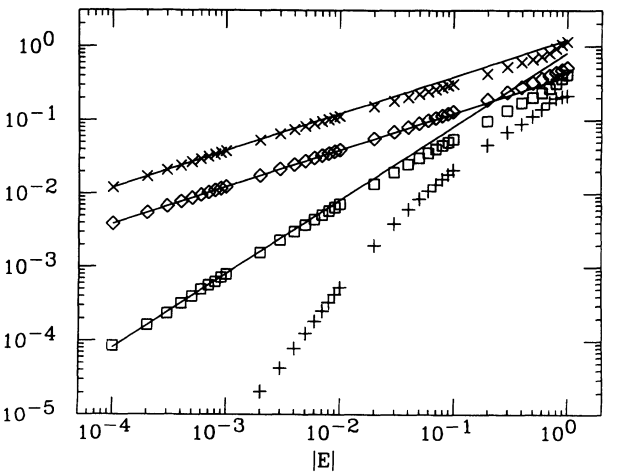

FIG. 6. Integrated density of states and inverse localization length for $\alpha=-2$. $\Diamond I_{\rm DOS}(E>0)/N$; $\Box L_{\rm ILL}(E>0)$; $+I_{\rm DOS}(E<0)/N$; $\times L_{\rm ILL}(E<0)$. The straight lines are the CEA predictions for the asymmetric distribution with $C_1=3C_2$, Eqs. (2.18)–(2.20).

$$1/J_c = \int_{-\infty}^{0} dJ\, P(J)/(J-W) + \int_{0}^{\infty} dJ P(J)/(J-W) , \tag{3.10}$$

with $W = iE^{1/2}J_c^{1/2}/2$, and assume the solution

$$1/J_c(E) = \langle J^{-1}\rangle + f(E) , \tag{3.11}$$

where $f(E)$ vanishes as $E \to 0$. Since the Greens function at small E varies as $-i(EJ_c)^{-1/2}$, the limiting value of the real part of J_c, $\langle J^{-1}\rangle^{-1}$, determines the density of states, whereas the imaginary part, $\mathrm{Im}f(E)$, is related to the inverse localization length. That is, we have

$$\begin{aligned} G_0(E) &= -(i/2)E^{-1/2}[\langle J^{-1}\rangle + f(E)]^{1/2} , \\ &\approx -(i/2)E^{-1/2}\langle J^{-1}\rangle^{1/2} \\ &\quad + (1/4)\,\mathrm{Im}f(E)\langle J^{-1}\rangle^{-1/2} + \ldots , \end{aligned} \tag{3.12}$$

where

$$\mathrm{Im}f(E) = x\int_{-\infty}^{\infty} dJ\, P(J)/(J^2+x^2) , \tag{3.13}$$

with $x = (E/2\langle J^{-1}\rangle)^{1/2}$.

Specializing to the distribution (3.9), one finds

$$\begin{aligned} \mathrm{Im}f(E) &= x^{-\alpha}(C_1+C_2)\int_0^{\infty} dy\, y^{-\alpha}/(y^2+1) , \\ &= (\pi/2)x^{-\alpha}(C_1+C_2)\csc[\pi(1-\alpha)/2] . \end{aligned} \tag{3.14}$$

By combining (3.14) with (3.12), one sees that when $-1 < \alpha < 0$, the inverse localization length for $E > 0$ is predicted to vary as $E^{(1-\alpha)/2}$, whereas the integrated density of states continues to vary as $E^{1/2}$, independent of α.

In order to test these predictions, we have carried out a series of calculations for $\alpha = -\frac{1}{2}$ with the results shown in Fig. 7. The straight lines were calculated from

$$I_{\mathrm{DOS}}(E>0) = 3^{1/2}\pi^{-1}E^{1/2} , \tag{3.15}$$

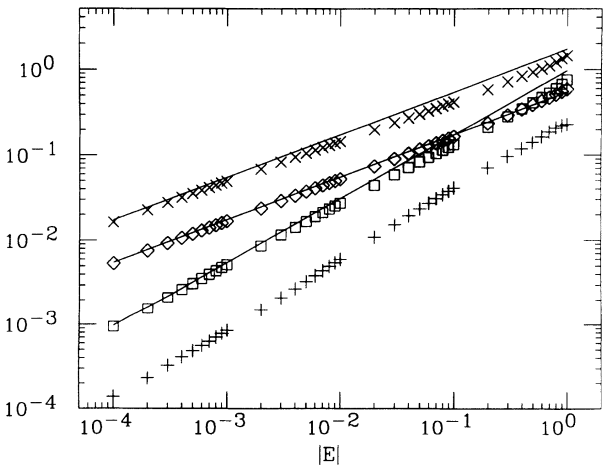

FIG. 7. Integrated density of states and inverse localization length for $\alpha = -\frac{1}{2}$. $\Diamond I_{\mathrm{DOS}}(E>0)/N$; $\Box L_{\mathrm{ILL}}(E>0)$; $+ I_{\mathrm{DOS}}(E<0)/N$; $\times L_{\mathrm{ILL}}(E<0)$. The straight lines are the CEA predictions for the asymmetric distribution with $C_1 = 3C_2$. Eqs. (3.15)–(3.17).

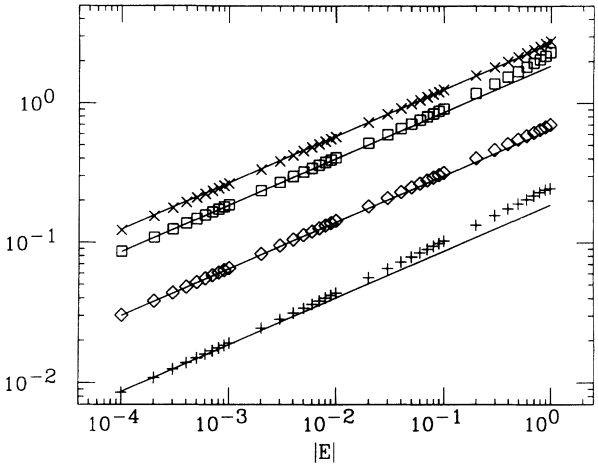

FIG. 8. Integrated density of states and inverse localization length for $\alpha = \frac{1}{2}$. $\Diamond I_{\mathrm{DOS}}(E>0)/N$; $\Box L_{\mathrm{ILL}}(E>0)$; $+ I_{\mathrm{DOS}}(E<0)/N$; $\times L_{\mathrm{ILL}}(E<0)$. The straight lines are the CEA results for the asymmetric distribution with $C_1 = 3C_2$, Eqs. (3.19)–(3.22).

$$L_{\mathrm{ILL}}(E>0) = \pi 2^{-1/2}3^{-3/4}E^{3/4} , \tag{3.16}$$

$$\begin{aligned} L_{\mathrm{ILL}}(E<0) &= \pi I_{\mathrm{DOS}}(-E)/N , \\ &= 3^{1/2}|E|^{1/2} , \end{aligned} \tag{3.17}$$

which are the CEA predictions for $\alpha = -\frac{1}{2}$ and $C_1 = 3C_2$. Once again, there is good agreement between the numerical data and the CEA.

Finally, when $0 < \alpha < 1$, one has $J_c \propto E^{\alpha/(2-\alpha)}$, where the coefficient of proportionality is a function of α and the ratio C_2/C_1. As a consequence, one finds

$$G_0(E) \sim E^{-1/(2-\alpha)}\exp[i\theta(\alpha, C_2/C_1)] . \tag{3.18}$$

From (3.18), it follows that $I_{\mathrm{DOS}}(E>0)$, $L_{\mathrm{ILL}}(E>0)$, $I_{\mathrm{DOS}}(E<0)$ and $L_{\mathrm{ILL}}(E<0)$ all vary as $E^{(1-\alpha)/(2-\alpha)}$ and that the results for $E<0$ are obtained from those for $E>0$ by making the replacement $\theta \to \theta - \pi/(2-\alpha)$. Figure 8 shows the numerical results for $\alpha = \frac{1}{2}$, $C_1 = 3C_2$, along with the predictions of the CEA:

$$I_{\mathrm{DOS}}(E>0)/N = 0.648E^{1/3} , \tag{3.19}$$

$$L_{\mathrm{ILL}}(E>0) = 1.851E^{1/3} , \tag{3.20}$$

$$I_{\mathrm{DOS}}(E<0)/N = 0.1864|E|^{1/3} , \tag{3.21}$$

$$L_{\mathrm{ILL}}(E<0) = 2.688|E|^{1/3} . \tag{3.22}$$

As in Figs. 1–7, there is good agreement between theory and simulation, especially at small $|E|$.

IV. DISCUSSION

The purpose of this paper has been to extend and generalize the earlier studies[1] of the dynamics of one-dimensional spin glasses in strong magnetic fields. In the analysis, particular emphasis was placed on the behavior of the integrated density of states and the inverse locali-

zation length near the precession frequency. The results of a calculation based on the coherent-exchange approximation were shown to be in good agreement with numerical simulation data for chains of 10^7 spins. The behavior of the system near the precession frequency was shown to depend on the average values of J^{-1} and J^{-2}. In the case of symmetric distributions of exchange interactions, where $\langle J^{-1}\rangle$ vanishes identically, so-called conventional behavior was obtained when $\langle J^{-2}\rangle$ was finite. In the conventional regime, the integrated density of states and the inverse localization length varied as $|E|^{2/3}$ with a coefficient that was proportional to $\langle J^{-2}\rangle^{1/3}$. The behavior in a regime where $\langle J^{-2}\rangle$ was infinite was investigated with a distribution of the form $P(J)\propto|J|^{-\alpha},\alpha<1$. For $-1<\alpha<1$, both the integrated density of states and the inverse localization length varied as $|E|^{(1-\alpha)/(2-\alpha)}$.

In the case of asymmetric distributions, when both $\langle J^{-1}\rangle$ and $\langle J^{-2}\rangle$ are finite and nonzero, the integrated density of states varied as $E^{1/2}$ and the inverse localization length as E with coefficients determined by the average values of J^{-1} and $J^{-2}(\langle J^{-1}\rangle>0)$. The inverse localization length for modes with $E<0$ was equal to the integrated density of states for $E>0$, apart from a factor of π, and thus varied as $|E|^{1/2}$. As long as $\langle J^{-1}\rangle$ is finite, the integrated density of states for $E>0$ and the inverse localization length for $E<0$ both vary as $|E|^{1/2}$, even when $\langle J^{-2}\rangle$ is infinite; however, the power dependence of the inverse localization length for modes with $E>0$ depends on the details of the interaction. For an asymmetric distribution where both $P(J>0)$ and $P(J<0)$ varied as $|J|^{-\alpha}$, it was found that the inverse localization length was proportional to $E^{(1-\alpha)/2}$ for $-1<\alpha<0$. For the same distribution with $0<\alpha<1$, the integrated density of states and the inverse localization length for both $E>0$ and $E<0$ varied as $|E|^{(1-\alpha)/(2-\alpha)}$.

The power-law behavior discussed above follows from an analysis based on the coherent-exchange approximation. As noted, however, the results from the CEA are in good agreement with the numerical data from chains of 10^7 spins, which suggest that the CEA is a very good approximation at small $|E|$. Additional evidence in support of this conjecture comes from I, where a connection is established between the high-field limit of the $\pm J$ model with equal concentrations of + and − bonds, the corresponding model in zero field, and the one-dimensional Schrödinger equation in a random potential proportional to E for which exact results have been obtained by Derrida and Gardner.[6] In the CEA, $I_{\rm DOS}(E)/N$ varies as $0.164|E|^{2/3}$, while $L_{\rm ILL}(E)=0.298|E|^{2/3}$; the equivalent results, obtained by applying the theory of Ref. 6, are $I_{\rm DOS}(E)/N=0.160|E|^{2/3}$ and $L_{\rm ILL}(E)=0.289|E|^{2/3}$.[1,7]

In the case of the nonsymmetric distributions, a comparison can be made with the exact results for the fully asymmetric distribution, $P(J)\propto J^{-\alpha}$, $J>0$; $P(J)=0$, $J<0$, which is the distribution for a ferromagnetic chain.[8] In this case, behavior in the high-field limit is identical to that in zero field, apart from a shift of H in the frequency scale. As noted elsewhere,[9] the eigenvalue distribution for the ferromagnetic chain is equivalent to that of the master equation with nearest-neighbor transfer rates equal to $J_{n,n+1}$. For the latter model, rigorous results for the limiting behavior of the distribution of eigenvalues have been obtained by Bernasconi, Schneider, and Wyss[10] and Schneider and Bernasconi.[11] In particular, the CEA results for the $I_{\rm DOS}$ with $\langle J^{-1}\rangle$ finite, Eq. (2.18) are in exact agreement with their calculations. In addition, the rigorous results for the power-law behavior of the integrated density of states when $\alpha>0, E^{(1-\alpha)/(2-\alpha)}$, are also reproduced in the CEA. The high-field dynamics of the Heisenberg spin glass with a fully asymmetric distribution of exchange interactions is also characteristic of the one-dimensional planar spin glass with dominant uniaxial anisotropy in *zero* field. A CEA theory developed for the latter model also gives a good agreement with simulation data.[12,13]

Next, we expand on the point made in I that the result for the $L_{\rm ILL}$ for asymmetric distributions in the conventional regime has the same form as that derived rigorously by Matsuda and Ishii[14] for an isotropically disordered chain with the dynamical equation

$$-m_n\omega^2u_n=K(u_{n+1}+u_{n-1}-2u_n)\ . \tag{4.1}$$

The corresponding inverse localization length is expressed as

$$L_{\rm ILL}(\omega^2)=(\langle m^2\rangle-\langle m\rangle^2)\omega^2/8K\langle m\rangle\ , \tag{4.2}$$

which is to be compared with Eq. (2.19).

Our final point concerns the CEA. The results obtained here, along with the findings reported in Refs. 1 and 5, are evidence that the coherent-exchange approximation provides a remarkably accurate characterization of the linearized magnon modes at high fields for spin glass models with random nearest-neighbor exchange interactions in one, two, and three dimensions. The challenge for the future, on one hand, is to develop comparable approximations for characterizing the spin dynamics of these models in zero field, and, on the other, to extend the high-field theory to cover more realistic situations where the spin glass behavior arises from random alloying with magnetic ions having different exchange interactions.

ACKNOWLEDGMENTS

The authors would like to thank Dr. Ibrahim Avgin for helpful comments. Research supported in part by the National Science Foundation under the Cooperative Agreement DMR-9212658.

*Also at Department of Physics, University of Wisconsin–Madison, Madison, WI 53706.

[1] I. Avgin and D. L. Huber, Phys. Rev. B **48**, 13 625 (1993).
[2] P. Dean, Proc. Phys. Soc. (London) **73**, 413 (1959).
[3] D. J. Thouless, J. Phys. C **5**, 77 (1972); Phys. Rep. **13**, 93 (1974).
[4] H. B. Rosenstock and R. E. McGill, J. Math. Phys. **3**, 200 (1962).
[5] I. Avgin, D. L. Huber, and W. Y. Ching, Phys. Rev. B **46**, 223

(1992); **48**, 16 109 (1993). For earlier applications of the CEA formalism, see R. A. Tahir-Kheli, *ibid.* B **6**, 2808 (1972); E-N. Foo and S. M. Bose, *ibid.* **9**, 347, 3944 (1974).

[6]B. Derrida and E. Gardner, J. Phys. (Paris) **45**, 1283 (1984).

[7]A. Boukahil and D. L. Huber, Phys. Rev. B **40**, 4638 (1989).

[8]The thermodynamic properties of Ising models with fully asymmetric distributions of exchange interactions of the form considered here were investigated by Cabib and Mahanti [D. Cabib and S. D. Mahanti, Progr. Theor. Phys. (Japan) **51**, 1030 (1974)].

[9]D. L. Huber, D. S. Hamilton, and B. Barnett, Phys. Rev. B **16**, 4642 (1977).

[10]J. Bernasconi, W. R. Schneider, and W. Wyss, Z. Phys. B **37**, 175 (1980).

[11]W. R. Schneider and J. Bernasconi, in *Mathematical Problems in Theoretical Physics,* Proceedings of the VI International Conference in Mathematical Physics, edited by R. Schrader, R. Seiler, and D. A. Uhlenbrock (Springer, Berlin, 1982), p. 389.

[12]D. L. Huber and W. Y. Ching, J. Phys. C **13**, 5579 (1980).

[13]C. M. Grassl and D. L. Huber, Phys. Rev. B **29**, 5193 (1984).

[14]H. Matsuda and K. Ishii, Prog. Theor. Phys. Suppl. **45**, 56 (1970).